PPr701 Project
Report
on

Graphene:
Electronic band structure and defects

Submitted by

P181211 **Gaurav Agarwal**

Under the guidance of

Prof. Vijay Singh,
UM-DAE-CBS & HBCSE, Mumbai

Department of Physical Sciences
Centre for Excellence in Basic Sciences (UM-DAE-CBS)
Mumbai, India - 400098

Semester 7, 2021

Acknowledgement

I wholeheartedly thank Prof. Vijay Singh, who agreed to guide me in an online mode, introduced me to the topic and provided me with the necessary guidance for this project. I thank him for his patience and reassurance which were showered on me in the project's entirety.
I would also like to thank my family and friends for their support.

Gaurav Agarwal

December, 2021
UM-DAE-CBS, Mumbai

Abstract

Graphene is one of the first 2-D materials to be discovered. We examine its physical structure and review the tight-binding model of Graphene with the next-nearest neighbour interaction. Only considering nearest neighbour hopping, we demonstrate the importance of Dirac points, the onset of the relativistic formulation and electrons acquiring pseudo-spin. We also show the e-h symmetry breaking on the inclusion of next-nearest hopping. Additionally, we derive the commonly stated density of states using Green's function. Further, we model substitutional impurities in the Graphene lattice by the Slater-Koster model and derive the change in the band structure.

Contents

Chapter 1

Introduction

1.1 History

Initially, 2D crystals were thought to be thermodynamically unstable. Landau and Mermin had even proposed accepted theoretical arguments for the instability. However, free-standing 2-D atomic crystals were first reported by Novoselov et al. in 2005 for the first time [1]. One of the crystals was a single-layer graphite sheet. Since then, numerous such 2D materials have been predicted and discovered. Recently, there has been a tremendous push to study 2-D materials with newer discoveries such as Borosene, Silicene, Boron-Nitride, and transition metal dichalcogenides.

Novoselov and Geim separated single layers of graphite - now called 'Graphene' - by mechanically cleaving a few layers of graphite with scotch tape and depositing them on a silicon substrate. The crystal was confirmed to be single-layered by atomic force microscopy. Both won the Nobel prize for this discovery. Graphene has since been subject to significant focus in nano-science [2], owing to its quirky properties like minimal electron scattering extending to micrometres, the existence of massless Dirac fermions showing signature anomalous integer quantum hall effect, or exploring analogues of fundamental physics.

1.2 Orbital structure

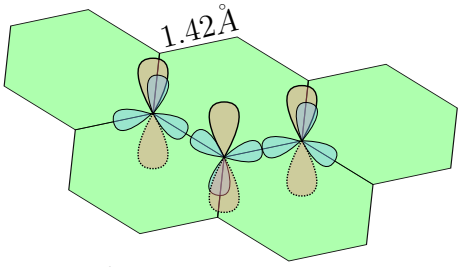

Graphene is simply a 2-D layer of graphite and has the same orbital structure as graphite. Carbon with an atomic number of 6 has an electronic configuration of $1s^2$ $2s^2$ $2p^2$. The outer shell can hybridize to form sp^2 molecular orbitals, thus giving it both s and p character.

This sp^2 nature also gives rise to a trigonal planar structure such that the σ bonds are in the plane. It gives graphene structural robustness and a high Young's modulus (2.4 ± 0.4 TPa). The sigma bonds are 1.42 $\mathring{A}$ in length and are filled. The p orbital perpendicular to the plane is half-filled and can form a π bond with the neighbouring atoms. We model this π electron as a free electron constrained on the lattice.

1.3 Lattice structure

The trigonal planar hybridization gives the lattice a honeycomb structure. The lattice is broken up into two different triangular lattices A and B (refer figure 1.1), superimposed on each other.
We can write the lattice translation vectors in the form of the lattice constant 'a' with the help of the figure 1.1.

$$a_1 = \frac{a}{2}(3, \sqrt{3}), \quad a_2 = \frac{a}{2}(3, -\sqrt{3}) \tag{1.1}$$

The three nearest neighbors vectors in real space are given by:

$$\delta_1 = \frac{a}{2}(1, \sqrt{3}), \quad \delta_2 = -a(1, 0), \quad \delta_3 = \frac{a}{2}(1, -\sqrt{3}) \tag{1.2}$$

In the reciprocal space, the reciprocal lattice vectors are given by:

$$b_1 = \frac{2\pi}{3a}(1, \sqrt{3}), \quad b_2 = \frac{2\pi}{3a}(1, -\sqrt{3}) \tag{1.3}$$

Finally, the Dirac points are given by:

$$K = \left(\frac{2\pi}{3a}, \frac{2\pi}{3\sqrt{3}a}\right), \quad K' = \left(\frac{2\pi}{3a}, -\frac{2\pi}{3\sqrt{3}a}\right) \tag{1.4}$$

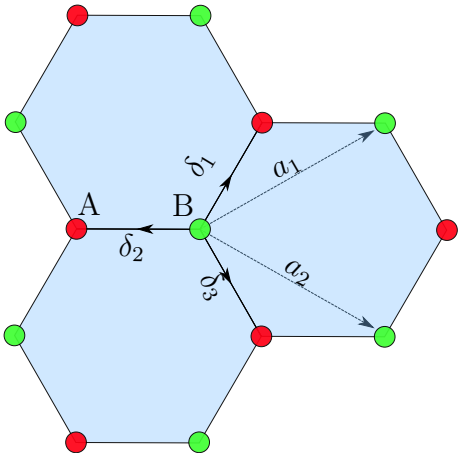

(a) The two triangular lattices superimposed on each other are shown in red and green labeled A and B. δ_i represents the translation vector required to jump from one lattice to another.

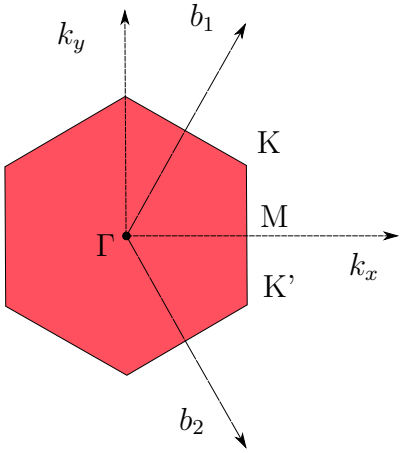

(b) The first Brillouin zone is shown in the reciprocal space $k_x - k_y$ with reciprocal lattice vectors b_i. K and K' are called the Dirac points and define the corners of Brillouin zone.

Figure 1.1

Chapter 2

Electronic Structure

The electronic structure of a solid material arises out of the ion potentials that electrons experience in the solid. The electronic structure explains electron transport, conduction, heat transfer, and multiple other phenomena in a material.

2.1 The tight-binding method

2.1.1 Background

The tight-binding approach of calculating the electronic band structure uses an approximate set of individual wave functions associated with atoms on each lattice site. This is like the LCAO approach, with the difference being that the electrons are assumed to be 'tightly bound' with their atoms and hence do not get affected by the bulk of the material, rather, only the nearest neighbours. The potential is added separately in a small term (ΔU) in addition to the original Hamiltonian. [3].

The wavefunctions are constructed as plane waves in accordance with the *Bloch condition*:

$$\psi_m(r + R_l) = e^{i\vec{k}.\vec{R_l}}\psi_m(r) \tag{2.1}$$

where R_l is the lattice translation vector.
For N atoms, the wavefunction is constructed as a linear combination of N such orbitals:

$$\psi_{mk}(r) = \sum_{R_n} e^{i\vec{k}.\vec{R_n}}\psi_m(r - R_n) \tag{2.2}$$

where $\vec{k}$ is the crystal momentum. We now introduce a potential such that the wavefunctions die before the potential becomes appreciable. This changes the wavefunctions slightly, and we approximately express it in an expansion of localized atomic wavefunctions. We assume these approximate wave functions to be $\phi(r)$. These are called *Wannier functions*.

$$\psi_{mk}(r) = \frac{1}{\sqrt{N}} \sum_{n}^{N} e^{i\vec{k}.\vec{R_n}}\phi(r - R_n) \tag{2.3}$$

It is clear from the normalized relation above that ϕ and ψ, i.e., the Wannier states and Bloch states, are the Fourier transforms of each other going from k space to position and vice-a-versa.

We can now substitute (2.3) in the Schrödinger equation, pre-multiply by one of the conjugate wavefunctions and integrate over space to get the band structure:

$$\int_r \psi_m^*(r) H \psi(r) dr = \int_r \psi_m^*(r)(H_{at} + \Delta U)\psi(r) dr \tag{2.4}$$

$$\Rightarrow \epsilon(k) \int_r \psi_m^*(r)\psi(r) dr = E_m \int_r \psi_m^*(r)\psi(r) dr + \int_r \psi_m^*(r)\Delta U \psi_m^*(r) dr \tag{2.5}$$

where $\epsilon(k)$ is the band structure. We can set E_m to be zero as it only acts as a constant in the system.

In the second quantized language, the wave function can be expressed as the product of operators 'a' multiplied by a complete set of scalar functions ϕ, given that the potential is independent of time.

$$\psi(r) = \sum_\lambda a_\lambda \phi_\lambda(r) \tag{2.6}$$

which means that the integral in RHS of equation (2.5) is modified as:

$$\int_r \psi^\dagger(r)(H_{at} + \Delta U)\psi^\dagger(r) dr \tag{2.7}$$

$$= \sum_{\lambda,\lambda'} \int_r a_\lambda^\dagger a_{\lambda'} \phi_\lambda^*(r)(H_{at} + \Delta U)\phi_{\lambda'}(r) dr \tag{2.8}$$

$$= \sum_{\lambda,\lambda'} a_\lambda^\dagger a_{\lambda'} E_{\lambda,\lambda'} \tag{2.9}$$

Here $a_\lambda^\dagger$ and a_λ are creation and annihilation operators such that $[a_\lambda^\dagger, a_{\lambda'}] = \delta_{\lambda,\lambda'}$ which are akin to ladder operators. This form allows the study of a localized picture of the electrons on the lattice without dealing with wavefunctions explicitly.

We can further simplify (2.9) by separating it between its diagonal elements representing on-site energies and other off-diagonal terms representing energy associated with electrons jumping to other orbitals, i.e. sites of other atoms. This jumping happens for bound electrons courtesy of quantum tunnelling.

Hence, the tight-binding Hamiltonian in the second quantized formulation is written as:

$$\mathcal{H} = E_o \sum_{\lambda,} a_\lambda^\dagger a_\lambda + \sum_{\substack{\lambda,\lambda' \\ \lambda \neq \lambda'}} a_\lambda^\dagger a_{\lambda'} E_{\lambda,\lambda'} \tag{2.10}$$

$$\text{where } E_o = \int_r \phi_\lambda^*(r)(H_{at} + \Delta U)\phi_\lambda(r) dr$$

2.1.2 Graphene band structure with tight-binding approximation

The tight-binding Hamiltonian for electrons in the Graphene lattice is written below with terms accounting for the nearest neighbour and the next nearest neighbour (NNN) interaction [4].:

$$\mathcal{H} = -t \sum_{\langle i,j\rangle,\sigma} \left(a^{\dagger}_{\sigma,i} b_{\sigma,j} + \text{ h.c. } \right) - t' \sum_{\langle\langle i,j\rangle\rangle,\sigma} \left(a^{\dagger}_{\sigma,i} a_{\sigma,j} + b^{\dagger}_{\sigma,i} b_{\sigma,j} + \text{ h.c. } \right) \tag{2.11}$$

where $a_{i,\sigma}$ and $a^{\dagger}_{i,\sigma}$ are the annihilation and creation operators acting on-site R_i on one of the sub-lattices. The hopping energy from one sub-lattice to another (i.e. the nearest neighbour) is denoted by t, whereas the next nearest neighbour hopping energy is denoted by t' and represents hopping within the same lattice. Units such as $\hbar$ have been omitted.
To derive the electronic band structure in terms of crystal momentum $\vec{k}$ we express the operators in position space as an inverse Fourier transform of operators in k space as follows:

$$\begin{aligned} a^{\dagger}_i &= \frac{1}{\sqrt{N/2}} \sum_k e^{i\vec{k}.\vec{r_i}} a^{\dagger}_k \\ b^{\dagger}_i &= \frac{1}{\sqrt{N/2}} \sum_k e^{i\vec{k}.\vec{r_i}} b^{\dagger}_k \end{aligned} \tag{2.12}$$

where N/2 is the number of lattice sites corresponding to one of the triangular lattices as shown in Figure (1.1).
For simplicity, we break the Hamiltonian in (2.11) into two parts, one representing nearest neighbour interaction t (I) and one representing next nearest neighbour interaction t' (II).

(I) *: Nearest neighbour terms*
Considering δ_i to be the nearest neighbor vectors (refer Figure (1.1)), we can write the indices of second lattice as $j = i + \delta_l$ where $l = 1, 2, 3$. Further, we expand the first term by using equations (2.12) and ignore the spins since they are not relevant here.

$$\begin{aligned} \mathcal{H}_{\mathcal{I}} &= -t \sum_{\langle i,j\rangle} \left(a^{\dagger}_i b_j + b^{\dagger}_j a_i \right) \\ &= \sum_{i\in A} \sum_{\delta} \left(a^{\dagger}_i b_{i+\delta} + b^{\dagger}_{i+\delta} a_i \right) \\ &= -\frac{t}{N/2} \sum_{i\in A} \sum_{\delta,\vec{k},\vec{k'}} \left[e^{i\left(\vec{k}-\vec{k'}\right)\cdot\vec{r_i}} e^{-i\vec{k'}\cdot\vec{\delta}} a^{\dagger}_k b_{k'} + \text{ h.c. } \right] \end{aligned}$$

We can get rid of the $\vec{r_i}$ dependence by using the fact that

$$\sum_{i\in A} e^{i(\vec{k}-\vec{k'})\cdot\vec{r_i}} = \frac{N}{2} \delta_{kk'}$$

which simply gives us:

$$\begin{aligned}\mathcal{H}_{\mathcal{I}} &= -t\sum_{\delta,\vec{k},\vec{k}'}\Big[\delta_{kk\prime}e^{-i\vec{k}'\cdot\vec{\delta}}a_k^\dagger b_{k'} + \text{ h.c. }\Big] \\ &= -t\sum_{\delta,\vec{k}}\Big[e^{-i\vec{k}\cdot\vec{\delta}}a_k^\dagger b_k + e^{i\vec{k}\cdot\vec{\delta}}b_k^\dagger a_k\Big] \end{aligned} \tag{2.13}$$

(II) *: Next nearest neighbour term*
Denoting the next nearest neighbor on the same triangular lattice by the lattice indices γ_l, we have $j = i + \gamma_l$ where $l = 1, 2, 3, 4, 5, 6$ for the six NNN. We expand the Hamiltonian the same as we did before:

$$\begin{aligned}\mathcal{H}_{\mathcal{II}} &= -t'\sum_{\langle\langle i,j\rangle\rangle,\sigma}\Big(a_{\sigma,i}^\dagger a_{\sigma,j} + b_{\sigma,i}^\dagger b_{\sigma,j} + \text{ h.c. }\Big) \\ &= -t'\sum_{i\in A}\sum_{\gamma}\Big(a_i^\dagger a_{(i+\gamma)} + b_i^\dagger b_{(i+\gamma)} + \text{ h.c. }\Big) \\ &= -\frac{t'}{\sqrt{N/2}}\sum_{i\in A}\sum_{k,k',\gamma}\Big(e^{i\vec{k}\cdot\vec{r_i}}e^{-i\vec{k}\prime\cdot(\vec{r_i}+\vec{\gamma})}a_k^\dagger a_{k'} + e^{i\vec{k}\cdot\vec{r_i}}e^{-i\vec{k}\prime\cdot(\vec{r_i}+\vec{\gamma})}b_k^\dagger b_{k'} + h.c.\Big) \\ &= -\frac{t'}{\sqrt{N/2}}\sum_{i\in A}\sum_{k,k',\gamma}\Big(e^{i(\vec{k}-\vec{k}')\cdot\vec{r_i}}e^{-i\vec{k}\prime\cdot\vec{\gamma}}a_k^\dagger a_{k'} + e^{i(\vec{k}-\vec{k}')\cdot\vec{r_i}}e^{-i\vec{k}\prime\cdot\vec{\gamma}}b_k^\dagger b_{k'} + h.c.\Big) \\ &= -t'\sum_{i\in A}\sum_{k,\gamma}e^{-i\vec{k}\cdot\vec{\gamma}}\Big(a_k^\dagger a_k + b_k^\dagger b_k\Big) + h.c. \end{aligned} \tag{2.14}$$

Hence, the total Hamiltonian in equation (2.11) after reconciliation with equation (2.13) and (2.14) becomes:

$$\mathcal{H} = -t\sum_{\delta,\vec{k}}\Big[e^{-i\vec{k}\cdot\vec{\delta}}a_k^\dagger b_k + e^{i\vec{k}\cdot\vec{\delta}}b_k^\dagger a_k\Big] - t'\sum_{i\in A}\sum_{k,\gamma}\Big[e^{-i\vec{k}\cdot\vec{\gamma}}\Big(a_k^\dagger a_k + b_k^\dagger b_k\Big) + h.c.\Big]$$

Converting the above into a matrix formulation for simplicity we have:

$$\mathcal{H} = \sum_k \begin{pmatrix} a_k^\dagger & b_k^\dagger \end{pmatrix}\begin{pmatrix}\Gamma & \Delta \\ \Delta^* & \Gamma\end{pmatrix}\begin{pmatrix} a_k \\ b_k\end{pmatrix} \tag{2.15}$$

$$\text{where } \Gamma = -t'\sum_{\gamma}(e^{i\vec{k}\cdot\vec{\gamma}} + e^{-i\vec{k}\cdot\vec{\gamma}}) = -2t'\sum_{\gamma}\cos\Big(\vec{k}\cdot\vec{\gamma}\Big), \tag{2.16}$$

$$\Delta = -t\sum_{\delta}e^{-i\vec{k}\cdot\vec{\delta}} \tag{2.17}$$

The characteristic equation comes out to be:

$$\begin{aligned}&(\Gamma-\lambda)^2 - (\Delta\Delta^*) = 0 \\ &\Rightarrow \lambda = \Gamma \pm \sqrt{(\Delta\Delta^*)}\end{aligned} \tag{2.18}$$

The NN and NNN interactions are represented separately by Δ and Γ. The eigenvalue (i.e. energy) contribution of both can be obtained by evaluating Δ and Γ separately. We start by evaluating Δ with the definition of δ_i as per figure (1.1) and equation (1.2)

$$\begin{aligned}
\Delta &= e^{i\vec{k}\cdot\delta_1} + e^{i\vec{k}\cdot\delta_2} + e^{i\vec{k}\cdot\delta_3} \\
&= e^{i\vec{k}\cdot\vec{\delta}_2}\left[1 + e^{i\vec{k}\cdot\left(\vec{\delta}_1-\vec{\delta}_2\right)} + e^{i\vec{k}\cdot\left(\vec{\delta}_3-\vec{\delta}_2\right)}\right] \\
&= e^{-ik_xa}\left[1 + e^{i3k_xa/2}e^{i\sqrt{3}k_ya/2} + e^{i3k_xa/2}e^{-i\sqrt{3}k_ya/2}\right] \\
&= e^{-ik_xa}\left[1 + e^{i3k_xa/2}\left(e^{i\sqrt{3}k_ya/2} + e^{-i\sqrt{3}k_ya/2}\right)\right] \\
&= e^{-ik_xa}\left[1 + 2e^{i3k_xa/2}\cos\left(\frac{\sqrt{3}}{2}k_ya\right)\right]
\end{aligned} \tag{2.19}$$

$$\begin{aligned}
\Rightarrow \Delta^*\Delta &= 1 + 4\cos^2\left(\frac{\sqrt{3}}{2}k_ya\right) + 2\cos\left(\frac{\sqrt{3}}{2}k_ya\right)\left(e^{i3k_xa/2} + e^{-i3k_xa/2}\right) \\
&= 3 + 2\cos\left(\sqrt{3}k_ya\right) + 4\cos\left(\frac{3ak_x}{2}\right)\cos\left(\frac{\sqrt{3}ak_y}{2}\right) \\
&\equiv 3 + f(k)
\end{aligned} \tag{2.20}$$

Similarly, to expand Γ which corresponds to the six next-nearest neighbours on the same sub-lattice, we take the vectors γ expressed in the form of δ_i as defined in figure (1.1):

$$\begin{aligned}
\Gamma &= \sum_\gamma \cos\left(\vec{k}\cdot\vec{\gamma}\right) \\
&= \cos\left(\vec{k}\cdot\vec{\gamma}_1\right) + \cos\left(\vec{k}\cdot\vec{\gamma}_2\right) + \cos\left(\vec{k}\cdot\vec{\gamma}_3\right) + \cos\left(\vec{k}\cdot\vec{\gamma}_4\right) + \cos\left(\vec{k}\cdot\vec{\gamma}_5\right) + \cos\left(\vec{k}\cdot\vec{\gamma}_6\right) \\
&= \cos\left[\vec{k}\cdot\left(\vec{\delta}_1 - \vec{\delta}_2\right)\right] + \cos\left[\vec{k}\cdot\left(\vec{\delta}_3 - \vec{\delta}_2\right)\right] + \cos\left[\vec{k}\cdot\left(\vec{\delta}_3 - \vec{\delta}_1\right)\right] + \cos\left[\vec{k}\cdot\left(\vec{\delta}_2 - \vec{\delta}_1\right)\right] \\
&\qquad + \cos\left[\vec{k}\cdot\left(\vec{\delta}_2 - \vec{\delta}_3\right)\right] + \cos\left[\vec{k}\cdot\left(\vec{\delta}_1 - \vec{\delta}_3\right)\right] \\
&= 2\left(\cos\left[\vec{k}\cdot\left(\vec{\delta}_1 - \vec{\delta}_2\right)\right] + \cos\left[\vec{k}\cdot\left(\vec{\delta}_2 - \vec{\delta}_3\right)\right] + \cos\left[\vec{k}\cdot\left(\vec{\delta}_3 - \vec{\delta}_1\right)\right]\right) \\
&= 2\left\{\cos\left[\vec{k}\cdot\left(\frac{3a}{2}, \frac{\sqrt{3}a}{2}\right)\right] + \cos\left[\vec{k}\cdot\left(-\frac{3a}{2}, \frac{\sqrt{3}a}{2}\right)\right] + \cos[\vec{k}\cdot(0, \sqrt{3a})]\right\} \\
&= 2\left\{\cos\left(\frac{3ak_x}{2} + \frac{\sqrt{3}ak_y}{2}\right) + \cos\left(-\frac{3ak_x}{2} + \frac{\sqrt{3}ak_y}{2}\right) + \cos\left(k_y\sqrt{3}a\right)\right\} \\
&= 2\left\{2\cos\left(\frac{3ak_x}{2}\right)\cos\left(\frac{\sqrt{3}ak_y}{2}\right) + \cos\left(\sqrt{3}ak_y\right)\right\} \\
&= f(k)
\end{aligned}$$

We can finally put everything back together to get the band structure from equation (2.18) to be,

$$\lambda = E_{\pm}(\mathbf{k}) = \pm t\sqrt{3 + f(\mathbf{k})} - t' f(\mathbf{k}), \tag{2.21}$$
$$f(\mathbf{k}) = 2\cos\left(\sqrt{3}k_y a\right) + 4\cos\left(\frac{\sqrt{3}}{2}k_y a\right)\cos\left(\frac{3}{2}k_x a\right)$$

The nearest neighbour hopping energy t is ~ 2.8eV. The next-nearest hopping energy is estimated to be $\in [0.02t, 0.2t]$ [4].

2.2 Features of the band structure

For understanding the features of the band structure, we ignore NNN interaction (i.e. the t' term) in equation (2.21). The band structure has symmetry around the z-axis, and both the bands are zero around the Dirac points K and K' (refer figure 1.1). It turns out that the charge neutrality plane passes through K and K' [5] and Graphene is a semi-metal.

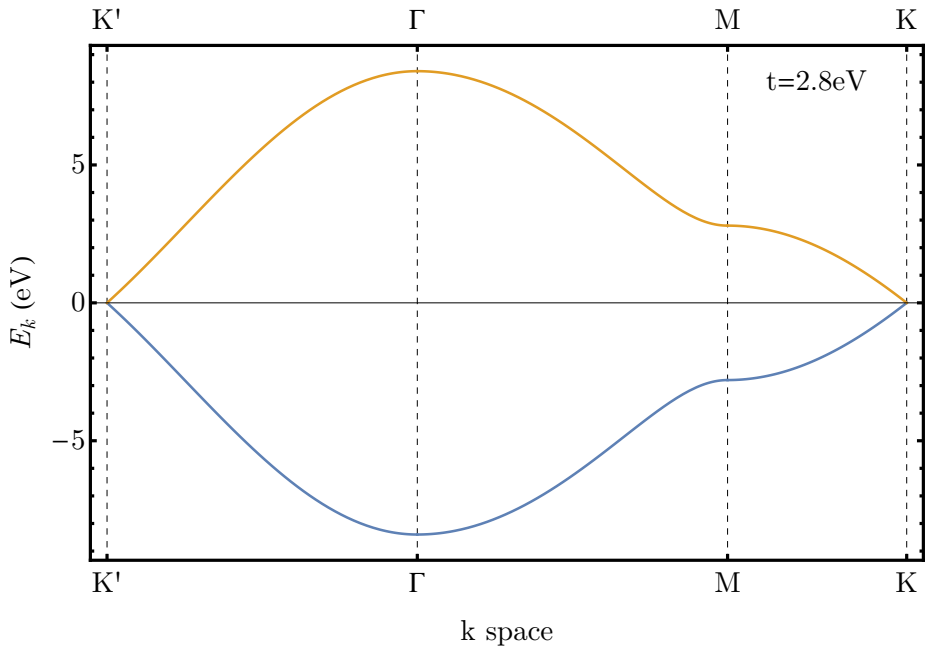

Figure 2.1: The band structure $E_{\pm}(k)$ (equation (2.21)) is shown. The conduction band (yellow) and valence band (blue) touch each other at the Dirac points K and K'. The NNN interaction is ignored as discussed above.

K and K' points in the reciprocal lattice are treated discordantly because they lie on different sub-lattices (figure 1.1). This is also reflected in the contour plot below (figure 2.2a), where the surface around the Dirac point is essentially rotated 180°.

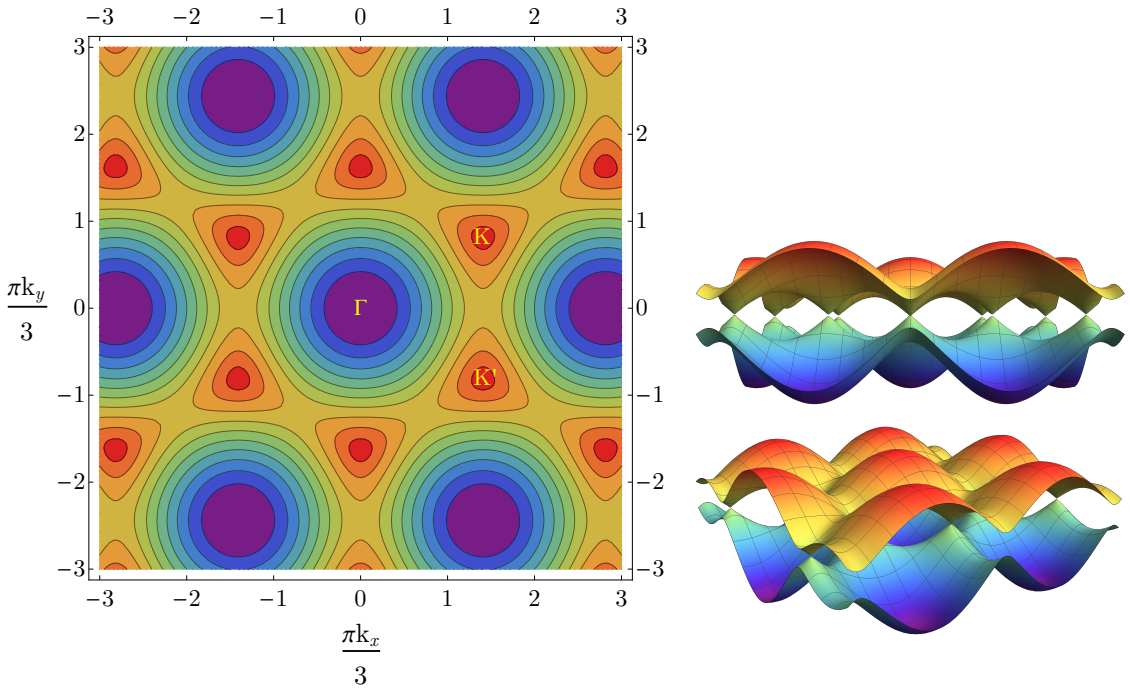

(a) (b)

Figure 2.2: The contour and 3D surface plots of the band structure $E_{\pm}(k)$ (equation (2.21)). The plot does not account for the NNN interaction i.e. the t' term. The conduction band (top) and valence band (bottom) touch each other at Dirac points. Graphene is a gap-less system.

2.2.1 Dirac points

The Dirac points are essential for analysis since the conduction and valence bands touch. As a result, electrons at K and K' do not require additional energy to jump from the valence band to the conduction band. Graphene, therefore, displays very high carrier mobility (see [6]). Analysis – as shown further – reveals that electrons have a linear dispersion relation around the Dirac point and act as ultra-relativistic particles. Due to this, they display a host of peculiar phenomena, particularly anomalous IQHE [4].

To derive the linear relation, we expand Δ equation (2.19) around K with the relative momentum $\vec{q} \equiv \vec{k} - \vec{K}$. Ignoring the t' i.e. NNN interaction for now, we get:

$$\begin{aligned}\Delta_{\mathbf{K+q}} &= e^{-iK_x a} e^{-iq_x a}\left[1 + 2e^{i3(K_x+q_x)a/2}\cos\left(\frac{\sqrt{3}\,(K_y+q_y)\,a}{2}\right)\right] \\ &= e^{-iK_x a} e^{-iq_x a}\left[1 - 2e^{3iaq_x/2}\cos\left(\frac{\pi}{3} + \frac{\sqrt{3}a}{2}q_y\right)\right]\end{aligned}$$

Taylor expanding the expression about $q = 0$ to first order, we have

$$\Delta_{K+q} = -ie^{-iK_x a}\frac{3a}{2}\left(q_x + iq_y\right) + O\left(\left(\frac{q}{K}\right)^2\right).$$

The band structure simply becomes:

$$\begin{aligned} E_{\pm}(K+q) &= \pm t\sqrt{\Delta_{\mathrm{K+q}}\Delta^{*}_{\mathrm{K+q}}} \\ &= \pm\frac{3at}{2}\sqrt{q_x^2+q_y^2} \\ &= \pm\frac{3at}{2}|\vec{q}| \end{aligned}$$

And hence,

$$E_{\pm}(\mathbf{q}) \approx \pm v_F|\mathbf{q}| + \mathcal{O}\left((q/K)^2\right) \qquad (2.22)$$

where v_F is the Fermi velocity ($\simeq 10^6$m/s).

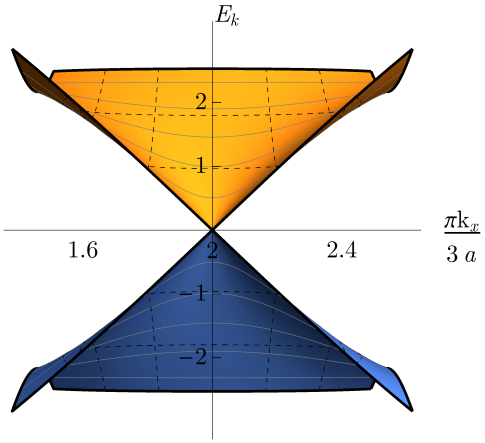

Figure 2.3: The Dirac cone centered at K.

The linear relation renders the band structure a symmetrical cone about the charge neutrality plane centered at the Dirac point. It is called the *Dirac cone*. The cone comes up as a feature in some similar 2D materials. We can express the Hamiltonian in (2.15) in the following form (without Γ, i.e. NNN interaction):

$$\hat{H}_{K+q} = v_F \begin{pmatrix} 0 & q_x + iq_y \\ q_x - iq_y & 0 \end{pmatrix}$$

We can introduce Pauli matrices and write the above as:

$$\begin{aligned} \hat{H}_{K+q} &= v_F\left(q_x\sigma_x - q_y\sigma_y\right) \\ \text{or, } \hat{H}_{K+q} &= v_F\overline{q}\cdot\hat{\sigma}. \end{aligned}$$

This is the form of ultra-relativistic massless fermions with 'v_F' instead of c, which is around 300 times smaller. The fermions behave as if they are mass-less. The relativistic behaviour has been a significant area of research interest in Graphene [4]. The linear dispersion has been experimentally observed, particularly in the Landau quantization in the magnetic field and the integer quantum Hall effect.

We treat ultra-relativistic electrons as quasi-particles and express their wavefunction can as per Dirac's fermions in QFT:

$$\begin{aligned} -i\hbar v_F\hat{\sigma}\nabla\psi(r) &= \epsilon\psi(r) \\ \text{where, } \psi^{\pm}(q) &= e^{iqr}\begin{pmatrix} e^{\chi i\theta_q/2} \\ \pm e^{i\theta_q/2} \end{pmatrix} \end{aligned}$$

where $\chi = \pm 1$ depending on the particle (electron/hole) and is called *chirality or helicity*. It is a pseudospin either parallel or antiparallel to $\vec{q}$. It should be noted that since the linear approximation only holds near the Dirac points, so does chirality as a quantum number. We can also differentiate between Dirac points by characterizing them with a valley index $\xi = \pm 1$. ξ can be incorporated into the Hamiltonian, and a new field of 'valleytronics' is born, where we can control the valley index due to the chiral nature of the fermions in Graphene [4].

The expansion of dispersion relation with the NNN interaction leads to the result [4]:

$$E_{\pm}(\mathbf{q}) \simeq 3t' \pm v_F|\mathbf{q}| - \left(\frac{9t'a^2}{4} \pm \frac{3ta^2}{8}\sin(3\theta_{\mathbf{q}})\right)|\mathbf{q}|^2,$$

where

$$\theta_{\mathbf{q}} = \arctan\left(\frac{q_x}{q_y}\right)$$

The inclusion of NNN interaction breaks the electron-hole symmetry (figure 2.4) as the Fermi level shifts below the Dirac point. The dispersion relation now depends on the direction of motion θ_q and has three-fold symmetry in the 2D space.

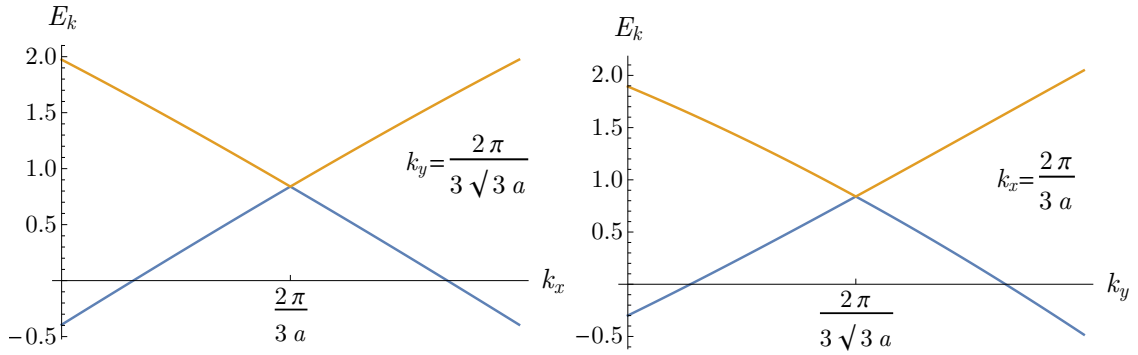

Figure 2.4: $(t' = 0.1t, t = 2.8eV)$As is evident, including t' makes the Fermi level go down into the conduction band (blue) and therefore breaks the e-h symmetry. The plots are zoomed in to the region of Dirac cones.

2.2.2 Cyclotron mass

We employ a lot of effective masses in solid-state physics such as conductivity, density-of-states, optical, and cyclotron mass. However, in the context of Graphene, the ultra-relativistic properties of Dirac fermions give us signature anomalous IQHE [2]. Hence, the magnetic response of electrons becomes of interest.

Electrons are defined to have an effective 'cyclotron' mass in the presence of a constant magnetic field. The part of crystal momentum k parallel to the field is a constant of motion. The part of k perpendicular to the field changes in time such that the electron moves in k-space in a closed line of constant energy. Therefore, the electron follows a spiral path whose projection on a plane perpendicular to the field is a closed path in the real space and k-space. We cannot use the usual dependence on the curvature of the dispersion as it is only valid for parabolic relations. The effective mass, in this case, is given by [3] :

$$m^* = \frac{\hbar^2}{2\pi}\left(\frac{\partial A(E)}{\partial E}\right)$$

Where $A(E)$ is the area bound by the closed path in $k_\perp$ space. In an isotropic material, the closed path is simply a circle and hence, $A(k) = \pi k^2$. Therefore, we can write:

$$m^* = \frac{\hbar^2}{2\pi}\frac{\partial A(k)}{\partial k}\frac{\partial k}{\partial E} = \hbar^2 k\left(\frac{\partial E}{\partial k}\right)^{-1} \tag{2.23}$$

On including the previously ignored $\hbar$, near the Dirac points the dispersion relation was: $E(k) \simeq \hbar v_F k$ (equation (2.22)). This leads to:

$$m^* = \frac{\hbar k}{v_F} \tag{2.24}$$

This value has been verified with cyclotron resonance measurements. If we inspect closely, equation (2.23) also suggests that the effective mass is, in this case, also the group velocity of the electron wave-packet.

2.3 The Density of States

The density of states is given by

$$\rho(E) = \frac{1}{N}\sum_{i=1}^{N}\delta(E - E(k_i))$$

and represents the density number of available states that can be occupied in a system. The density of states can often be represented in the form of Green's function which is given by:

$$\hat{G}(E) = \frac{1}{E\hat{I} - \hat{H}}$$

such that $\mathcal{H}\psi = E\psi \Rightarrow \hat{G}\psi = 0$. We can further change the above expression by expanding in the Bloch space:

$$\begin{aligned}\hat{G}(E) &= \sum_k \frac{|k\rangle\langle k|}{E\hat{I} - \hat{H}} \\ &= \sum_k \frac{|k\rangle\langle k|}{E - \epsilon_k}\end{aligned}$$

Taking a projection on Wannier basis, we get:

$$\langle n|\hat{G}(E)|n\rangle = \frac{1}{N}\sum_k \frac{1}{E\hat{I} - \epsilon_k} \equiv \hat{G}_{nn}(E)$$

which represents the diagonal Green's function, also called the 'locator'.

$$\Rightarrow -\frac{1}{\pi}\mathrm{Im}\left[\hat{G}_{nn}(E)\right] = -\frac{1}{N\pi}\mathrm{Im}\sum_k \frac{1}{E\hat{I} - \epsilon_k}$$

But, $\lim_{\eta\to 0}\frac{1}{x\pm i\eta} = \mathrm{Pr}\left[\frac{1}{x}\right] \mp i\pi\delta(x)$ (Plemelj Rule)

$$\begin{aligned}\Rightarrow -\frac{1}{\pi}\mathrm{Im}\left[\hat{G}_{nn}(E)\right] &= \frac{1}{N}\sum_k \delta(E - \epsilon_k) \\ &= \rho(E)\end{aligned} \tag{2.25}$$

We will employ this definition to derive the density of states of Graphene.

2.3.1 Derivation

We will derive an expression that is often left unverified in literature. It was first stated without proof by Hobson and Nirenberg in 1953 [7] and has been used time and time again, including the primary reference for this report [4, Neto et al. 2009]. From equation (2.21) we have the following expression for the band structure:

$$\epsilon_{\pm}(k) = \pm t\sqrt{3 + \cos\left(\sqrt{3}k_y a\right) + 4\cos\left(\frac{\sqrt{3}}{2}k_y a\right)\cos\left(\frac{3}{2}k_x a\right)} \tag{2.26}$$

Consequently, the corresponding Green's function would be:

$$G(E) = \frac{1}{E-\hat{H}} = \sum_k \frac{\langle k|k\rangle}{E-\hat{H}} = \sum_k \left[\frac{\langle k|k\rangle}{E-\epsilon(k)} + \frac{\langle k|k\rangle}{E+\epsilon(k)}\right]$$
$$\Rightarrow G(E) = 2E\sum_k \frac{\langle k|k\rangle}{E^2-\epsilon(k)^2} \tag{2.27}$$

Converting the summation in (2.27) to an integral over the first Brillouin zone as specified by the reciprocal vectors $\vec{b_i}$ in equation (1.3) as $k_x \in \left[\frac{-2\pi}{3a}, \frac{2\pi}{3a}\right]$ and $k_y \in \left[\frac{-2\pi}{\sqrt{3}a}, \frac{2\pi}{\sqrt{3}a}\right]$ we have:

$$G(E) = \frac{2E}{\Delta k}\int_{B.Z.} \frac{d^2k}{E^2-\epsilon(k)^2}$$

where $\Delta k = \Delta k_x \times \Delta k_y = \frac{4\pi^2}{3\sqrt{3}a^2}$ Here we have :

$$G(E) = \frac{2E}{\Delta k}\int_{\frac{-2\pi}{3a}}^{\frac{+2\pi}{3a}} dk_x \int_{\frac{-2\pi}{\sqrt{3}a}}^{\frac{+2\pi}{\sqrt{3}a}} \frac{dk_y}{E^2-\epsilon(k)^2} = \frac{2E}{\Delta k} \times \frac{4}{3\sqrt{3}a^2}\int_{-\pi}^{\pi} dx \int_{-\pi}^{\pi} \frac{dy}{E^2-\epsilon(k)^2}$$

(making the variable change $k_x \to x, k_y \to y$)
Substituting from (2.26) and Δk we have:

$$G(E) = \frac{2E}{\pi^2}\int_{-\pi}^{\pi} dy \int_{-\pi}^{\pi} \frac{dx}{E^2 - t^2[3+\cos(2y)+4\cos(y)\cos(x)]}$$
$$= \frac{2E}{\pi^2 t^2}\int_{-\pi}^{\pi} dy \int_{-\pi}^{\pi} \frac{dx}{\left(\frac{E^2}{t^2}-3\right) - 2\cos(2y) - 4\cos(y)\cos(x)}$$

To make the expression less strenuous we define $\left(\frac{E^2}{t^2}-3\right) = \epsilon^2 - 3 \equiv \tau$:

$$G(E) = \frac{2E}{\pi^2 t^2}\int_{-\pi}^{\pi} dy \int_{-\pi}^{\pi} \frac{dx}{(\tau - 2\cos(2y)) - 4\cos(y)\cos(x)}$$

This is a simple integral of the form below taken from [8, 2.553 integral type]

$$\int \frac{dx}{a+b\cos(x)} = \frac{2}{\sqrt{a^2-b^2}}\frac{\operatorname{atan}(x/2)}{a+b}$$

$$\Rightarrow G(E) = \frac{2E}{\pi^2 t^2}\int_{-\pi}^{\pi} dy \times \frac{\pi}{[(\tau - 2\cos(2y))^2 - 16\cos^2(y)]^{1/2}}$$
$$= \frac{2E}{\pi t^2}\int_{-\pi}^{\pi} \frac{dy}{[(\tau - 2\cos(2y))^2 - 16\cos^2(y)]^{1/2}}$$

This integral can be converted to an elliptical form to arrive at the commonly stated form in [4, Neto et al.]. To get near this form, we use the fact that $\cos(y)$ is an even function and therefore the integral must be the same from $[-\pi, 0]\&[0, \pi]$. Further, we make the variable change $y \to y/2$ to get:

$$G(E) = \frac{2E}{\pi t^2}\int_{0}^{\pi/2} \frac{dy}{[(\tau - 2\cos(y))^2 - 16\cos^2(y/2)]^{1/2}}$$
$$= \frac{2E}{\pi t^2}\int_{0}^{\pi/2} \frac{dy}{[(\tau - 2\cos(y))^2 - 8(\cos(y) + 1)]^{1/2}}$$

Substituting $\cos(y) = l$ we have:

$$G(E) = \frac{2E}{\pi t^2}\int_{0}^{1} \frac{dl}{[\tau^2 + 4l^2 - 4l\tau - 8l - 8]^{1/2}[1 - l^2]^{1/2}}$$

Factorizing the denominator further we have:

$$\tau^2 + 4l^2 - 4l\tau - 8l - 8 = \left(l - \frac{2 + \tau + 2\sqrt{\tau + 3}}{2}\right)\left(l - \frac{2 + \tau - 2\sqrt{\tau + 3}}{2}\right)$$
$$= \left(l - \frac{\epsilon^2 - 1 - 2\epsilon}{2}\right)\left(l - \frac{\epsilon^2 - 1 + 2\epsilon}{2}\right), \qquad \text{where } \epsilon = \left|\frac{E}{t}\right|.$$

$$\Rightarrow G(E) = \frac{2E}{\pi t^2}\int_{0}^{1} \frac{dl}{[(l - \frac{\epsilon^2-1-2\epsilon}{2})(l - \frac{\epsilon^2-1+2\epsilon}{2})(l-1)(l-(-1))]^{1/2}}$$

This allows us to use yet another integral from [8, Rhyzik, 3.147.3]:

$$\int_c^u \frac{dx}{\sqrt{(a-x)(b-x)(c-x)(x-d)}} = \frac{2}{\sqrt{(a-c))(b-d)}} K\left(\sqrt{\frac{(a-b)(c-d)}{(a-c)(b-d)}}\right)$$
$$\text{given } a > b > c > u \geq d.$$

This condition is satisfied by the following substitutions:

$$u = 0,\ c = 1,\ d = -1,\ a = \frac{\epsilon^2 - 1 + 2\epsilon}{2},\ b = \frac{\epsilon^2 - 1 - 2\epsilon}{2}$$

and therefore, our integral becomes:

$$G(E) = -\frac{2E}{\pi t^2} \times \frac{1}{\sqrt{(\epsilon - 1)^3(\epsilon + 3)}} K\left(\sqrt{\frac{16\epsilon}{(\epsilon - 1)^3(\epsilon + 3)}}\right) \tag{2.28}$$

Now the argument for the elliptic integral becomes complex if $0 \leq \epsilon < 1$ and real for $1 < \epsilon \leq 3$.
For the case of $0 \leq \epsilon < 1$ using [9, see 19.7.5, Imaginary-Modulus Transformation] we have:

$$K(ik) = \frac{1}{\sqrt{1+k^2}} K\left(\frac{k}{\sqrt{1+k^2}}\right)$$

where

$$k = \sqrt{\frac{16\epsilon}{(1-\epsilon)^3(\epsilon+3)}} \Rightarrow \frac{1}{\sqrt{1+k^2}} = \sqrt{\frac{(1-\epsilon)^3(\epsilon+3)}{(3-\epsilon)(\epsilon+1)^3}} \Rightarrow \frac{k}{\sqrt{1+k^2}} = \sqrt{\frac{16\epsilon}{(3-\epsilon)(\epsilon+1)^3}}$$

The density of states in terms of Green's function is given by:

$$n(E) = \frac{-1}{\pi}\mathrm{Im}(G(E))$$

Hence for the case of $0 \leq \epsilon < 1$ we get :

$$n(E) = \frac{4E}{\pi^2 t^2} \frac{1}{\sqrt{(3-\epsilon)(\epsilon+1)^3}} K\left(\sqrt{\frac{16\epsilon}{(3-\epsilon)(\epsilon+1)^3}}\right), \qquad 0 \leq \epsilon < 1 \qquad (2.29)$$

For the case of $1 < \epsilon \leq 3$ we need to get the imaginary part of an elliptic integral with real argument. We use [9, see 19.7.3, Legendre's Relations] which states:

$$K\left(\frac{1}{k}\right) = \frac{1}{k}\left(K\left(\frac{1}{k}\right) \pm iK\left(\sqrt{1-\frac{1}{k^2}}\right)\right)$$

to get:

$$n(E) = \frac{4E}{\pi^2 t^2} \frac{1}{\sqrt{(3-\epsilon)(\epsilon+1)^3}} K\left(\sqrt{\frac{(3-\epsilon)(\epsilon+1)^3}{16\epsilon}}\right), \qquad 1 < \epsilon \leq 3 \qquad (2.30)$$

Therefore, we finally have the density of states as:

$$\rho(E) = \frac{4}{\pi^2}\frac{|E|}{t^2}\frac{1}{\sqrt{Z_0}} F\left(\frac{\pi}{2}, \sqrt{\frac{Z_1}{Z_0}}\right) \qquad (2.31)$$

$$Z_0 = \begin{cases} \left(1+\left|\frac{E}{t}\right|\right)^2 - \frac{1}{4}\left[\left(\frac{E}{t}\right)^2 - 1\right]^2; & -t \leq E \leq t \\ 4\left|\frac{E}{t}\right|; & -3t \leq E \leq -t \vee t \leq E \leq 3t \end{cases}$$

$$Z_1 = \begin{cases} 4\left|\frac{E}{t}\right|; & -t \leq E \leq t \\ \left(1+\left|\frac{E}{t}\right|\right)^2 - \frac{1}{4}\left[\left(\frac{E}{t}\right)^2 - 1\right]^2; & -3t \leq E \leq -t \vee t \leq E \leq 3t \end{cases}$$

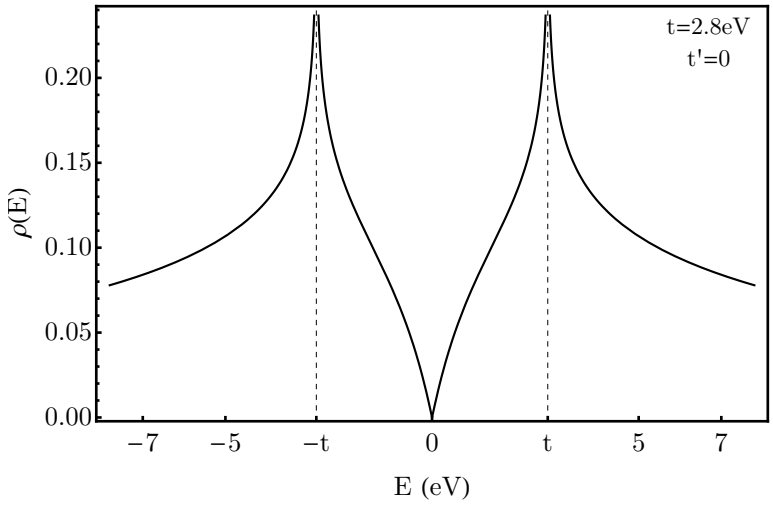

Figure 2.5: Density of states plotted as from equation (2.31). The density has a singularity at the NN hopping energy.

However, the reason this expression is avoided in literature is because of the fact that the main region of interest is in and around the Dirac point as discussed in section 2.2.1 and 2.2.2. Fortunately, the dispersion relation (2.22) results in a density of states:

$$\rho(E) = \frac{3\sqrt{3}a^2}{\pi}\frac{|E|}{v_F} \tag{2.32}$$

which is simply a scaled modulus function and is relatively undemanding in calculations.

Evaluating the density of states involves dealing with singularities at band energies (equation (2.27)). Analytically evaluating the density of states – even with the NN term – is tedious. It is helpful and sometimes required to use a numerical calculation of the density of states. We, therefore, need a numerical method that allows for the calculation of singular integrals. Fortunately, a modified version of Simpson's method (inspired from [10]) can be employed to evaluate the integral. The method and code are mentioned in the Appendix A.1.

Chapter 3

Substitutional Defects

It is almost impossible to get pure crystals in nature and otherwise. Therefore, modelling defects in a crystal structure is of importance. It also allows us to engineer materials and tune their qualities by doping impurities. Specifically, in the context of Graphene, the addition of impurities can alter the Fermi level to go above or below the Dirac points. Substitutional impurities in Graphene could be any similar-sized element such as Boron or Nitrogen. One of the ways to model impurities is by the Slater-Koster method.

3.1 The Slater-Koster Model

The following method was first proposed as a simplification for defects for the LCAO approach by Slater and Koster in 1954 [11]. It is now referred to as the 'SK' model in the literature.
Let us consider a tight-binding approximation with a localized substitutional impurity. We write the Hamiltonian of the system as $\mathcal{H} = H_o + V$, where H_o is the unperturbed Hamiltonian corresponding to the system free of defects. V is the potential induced by the localized impurity. The Green's function is given by

$$\hat{G}(E) = \frac{1}{E\hat{I} - \hat{\mathcal{H}}} = \sum_{\lambda} \frac{|\lambda\rangle \langle\lambda|}{E - \epsilon_\lambda}$$

where λ represents the eigenstate. Writing the above in the form of a matrix:

$$G = \begin{pmatrix} \lambda_1 \\ \lambda_2 \\ \vdots \\ \lambda_n \end{pmatrix} \begin{pmatrix} \frac{1}{E-\epsilon_{\lambda_1}} & 0 & \dots & 0 \\ 0 & \frac{1}{E-\epsilon_{\lambda_2}} & \dots & 0 \\ \vdots & & & \vdots \\ 0 & 0 & \dots & \frac{1}{E-\epsilon_{\lambda_n}} \end{pmatrix} \begin{pmatrix} \lambda_1 & \lambda_2 & \dots & \lambda_n \end{pmatrix}$$

$$\Rightarrow \text{Det } \hat{G} = \prod_{\lambda} \frac{1}{E - \epsilon_\lambda}$$

$$\Rightarrow \log\Big(\text{Det } \hat{G}\Big) = -\log\left(\prod_{\lambda} \frac{1}{E - \epsilon_\lambda}\right) \tag{3.1}$$

Now before proceeding further, it is best to break the Hamiltonian into the unperturbed H_o and the perturbation V with the aim of expressing $G\hat{(E)}$ in the form of the unperturbed Green's function $G_o = 1/(E - \epsilon_\lambda)$ such that the defect can be modeled without explicitly including the impurity state.

$$\begin{aligned} G(E) &= \frac{1}{E - H_o - V} = \frac{1}{(E - H_o)\left(1 - (E - H_o)^{-1} V\right)} \\ &= \left[(E - H_o)\left(1 - (E - H_o)^{-1} V\right)\right]^{-1} \\ &= \left(1 - (E - H_o)^{-1} V\right)^{-1} (E - H_o)^{-1} \\ &= (1 - G_o(E)V)^{-1} G_o(E) \end{aligned}$$

On expansion with Taylor series, we have:

$$\begin{aligned} G(E) &= G_o(E) + G_o(E)VG_o(E) + G_o(E)VG_o(E)VG_o(E) + \ldots \\ &= G_o(E) + G_o(E)V\left[G_o(E) + G_o(E)VG_o(E) + \ldots\right] \\ &= G_o(E) + G_o(E)VG(E) \\ &\Rightarrow \frac{G}{G_o} = (1 - VG_o)^{-1} \end{aligned} \tag{3.2}$$

Now, the density of states as in (2.25) is given by:

$$\begin{aligned} \rho(E) &= \frac{-1}{\pi}\mathrm{Im}(G(E)) = \frac{-1}{\pi}\mathrm{Im}\left(\sum_\lambda \frac{1}{E - \epsilon_\lambda}\right) \\ &= \frac{-1}{\pi}\mathrm{Im}\left[\sum_\lambda \frac{d}{dE}(\log(E - \epsilon_\lambda))\right] \\ &= \frac{-1}{\pi}\mathrm{Im}\left[\sum_\lambda \frac{d}{dE}(\log(E - \epsilon_\lambda))\right] \end{aligned}$$

Using (3.1) we have:

$$\rho(E) = \frac{1}{\pi}\mathrm{Im}\left[\frac{d}{dE}(\log(\mathrm{Det}G))\right]$$

On the inclusion of the impurity, the density of states would change. Let this change be $\delta\rho(E) = \rho(E) - \rho_o(E)$ where ρ_o corresponds to the host density of states. Then, using equation (2.21) and the result above we have:

$$\begin{aligned} \delta\rho(E) = \rho(E) - \rho_o(E) &= \frac{-1}{\pi}\mathrm{Im}G(E) - \frac{-1}{\pi}\mathrm{Im}G_o(E) \\ &= \frac{-1}{\pi}\frac{d}{dE}\mathrm{Im}\left[\log(\det G) - \log(\det G_o)\right] \\ &= \frac{1}{\pi}\frac{d}{dE}\mathrm{Im}\left[(1 - VG_o)\right] \end{aligned}$$

We can redefine the above as:

$$\delta\rho(E) = \frac{1}{\pi}\frac{d\delta(E)}{dE},$$
$$\text{where } \delta(E) = \operatorname{atan}\left(\frac{\operatorname{Im}\left[\operatorname{Det}(1 - G_o V)\right]}{\operatorname{Re}\left[\operatorname{Det}(1 - G_o V)\right]}\right)$$

Since the impurity is localized, V is a 1×1 matrix and we can simply drop the determinant i.e. $\operatorname{Det}(V) \equiv u$. Taking $G_o = R_o(E) + iI_o(E)$ and considering the resonant energy level (the energy at which $\delta\rho$ is centered) to be E_R we have:

$$\delta(E) = -\operatorname{atan}\left(\frac{uI_o(E)}{1 - uR_o(E)}\right)$$
$$\Rightarrow \delta(E_R) \simeq -\operatorname{atan}\left(\frac{uI_o(E_R)}{1 - uR_o(E_R) - u(E - E_R)R_o'(E_R)}\right)$$

Taking $1 - uR_o(E_R) = 0$ to locate the resonant level we have:

$$\delta(E) = \operatorname{atan}\left(\frac{I_o(E_R)}{(E - E_R)R_o'(E_R)}\right)$$

$$\Rightarrow \delta\rho(E) = \frac{1}{\pi}\frac{d}{dE}\delta(E) = \frac{1}{\pi}\frac{d}{dE}\operatorname{atan}\left(\frac{I_o(E_R)}{(E - E_R)R_o'(E_R)}\right)$$
$$= \frac{1}{2\pi}\frac{\Gamma}{(E - E_R)^2 + \Gamma^2} \tag{3.3}$$
$$\text{where } \Gamma = \frac{2I_o(E_R)}{R_o'(E_R)}$$

This final result gives us the change in density of states of the material in the form of the material's unperturbed quantities. The change in density of states $\delta\rho$ can be added to the host density of states ρ_o to get the final density of states. This model is generally applied to semiconductors; however, we will apply it to Graphene in the next section.

3.2 Slater-Koster model on Graphene

The density of states as seen in figure 2.5 is very demanding to model. However, we can simplify the model by only using the shape of the DOS. We can approximate the DOS to be an 'M' shape given by:

$$\rho(x) = \rho_m \begin{cases} 0, & |x| > 3, \\ |x|^{-1}, & 1 < |x| \leq 3, \\ |x|, & |x| \leq 1. \end{cases} \tag{3.4}$$

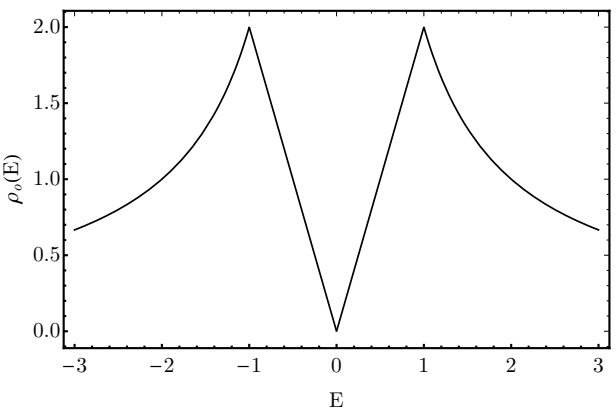

The M model can capture most of the qualitative features and can be scaled appropriately to capture the density of states around Dirac points exactly [12].
We start by writing the Green's function in terms of DOS:

$$\begin{aligned} \hat{G(E)} &= \frac{1}{N}\sum_{\lambda}\frac{1}{E-\epsilon_\lambda} \\ &= \frac{1}{N}\sum_{\lambda}\int\frac{\delta(z-\epsilon_\lambda)}{E-z}dz \\ &= \int\frac{\rho(z)}{E-z}dz = \frac{1}{\pi}\int_{-\infty}^{\infty}\frac{\mathrm{Im}G(z)}{E-z}dz \end{aligned} \tag{3.5}$$

From the Slater-Koster model, the resonant energy is given by $1 - uR_o(E_R) = 0$. Hence,

$$\mathrm{Re}G(E_R) = \frac{1}{U}$$

where U is the localized defect potential. E_R corresponds to the defect level energies in the system and can be solved numerically.
By substituting (3.4) into (3.5) and evaluating the integral we arrive at:

$$\hat{G}(E) = \rho_m E\log\left(\frac{E^2}{1-E^2}\right) + \frac{\rho_m}{E}\log\left(\frac{1-E^2}{1-(E/3)^2}\right)$$

The defect DOS then becomes:

$$\rho_d(E) = \frac{\rho_o(E)}{[1-U\,\mathrm{Re}\,G(E)]^2 + [\pi U\rho_o(E)]^2}$$

which gives us the density of states.
It should be pointed out that as U increases, the defect density of states spikes around the Dirac point. Doping Graphene with Nitrogen at 0.6% makes the Dirac point go below the Fermi level by 0.3eV[13]. This means that there are free electrons in the conduction band even at temperatures very close to zero.

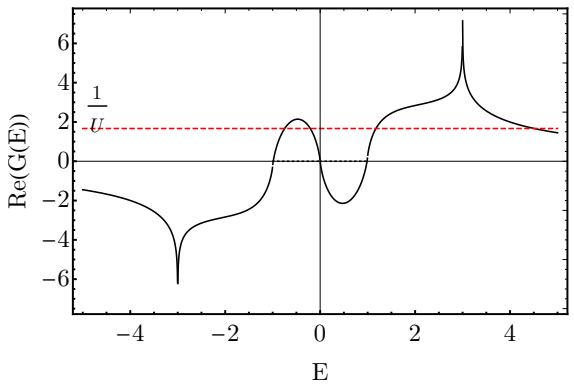

(a) The real part of Green's function is shown with a 1/U line. The intersection marks the resonant energy level E_R

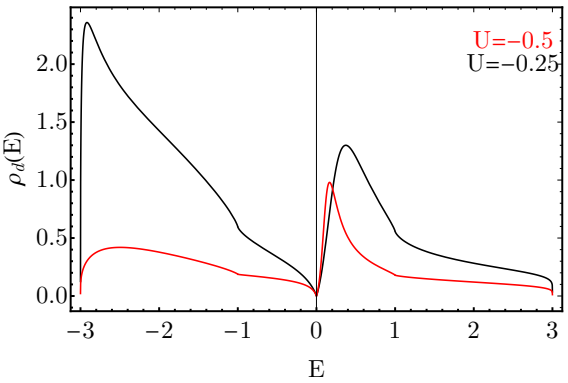

(b) The defect density of states is shown for different U values. Since G(E) is an odd function, the graph simply flips about y-axis if U is positive.

Chapter 4

Conclusion

We started by defining Graphene's lattice and explaining its planar structure. Graphene has high tensile strength due to in-plane sigma bonds. We explored the tight-binding approximation and applied it to Graphene to explain its band structure. Experiments verify the band structure we get. While ignoring the next nearest neighbour interaction, we found that the band structure is symmetric about the energy axis and zero at Dirac points (2.26). We also proved that the electrons show a linear dispersion relation around the Dirac points (2.22). This linear dispersion relation means that relativistic formulation becomes important since electrons behave as if they were massless. They also acquire pseudo-spins near the Dirac points called chirality. We explained the importance of measuring the magnetic response of electrons and, consequently described the cyclotron mass.

Further, we discovered the breaking of electron-hole symmetry on including the next-nearest neighbour interaction. We found a three-fold symmetry in the space called the trigonal warping of the electronic spectrum [4]. We moved on to derive the density of states, which is not established well in the literature, even though commonly stated (2.31). The derivation made use of elliptic integrals and gave us figure 2.5. We also derived an analytically convenient DOS around the Dirac points (2.32).

We described the Slater-Koster model, which models localized substitutional defects. We applied the SK model to Graphene, considering it free-standing and unaffected by the substrate. The Slater-Koster model yields the change in the density of states. Depending on the defect potential 'U', the defect density of states has peaks towards the end of the spectrum or near the Dirac point. Tweaking this value would allow us to play with the density of states and electronic properties of Graphene. This concludes our analysis of Graphene for the project report.

Work I intend to do

Some work can still be done to gain better insight into this project which spanned four months. Firstly, one can perform an analysis of DOS employing the numerical method and code mentioned in the appendix A.1. It would allow us to confirm our analytical result of DOS and obtain a result for DOS with NNN interaction. Further, we can study the disordered Anderson model for substitutional defects,

which renders 'pinning' of the defect DOS at the Dirac point [12].

Direction of active research

Research into 2-D materials is a highly active field. However, limiting ourselves to Graphene, the scientific community had initially been enamoured with the electronic properties of mono-layer Graphene. Its quirky electronic structure led to relativistic condensed matter physics, where phenomena very hard to observe in high-energy physics can be mimicked in a small lab[2]. Dirac Points also gave rise to an exciting field called 'valleytronics'[4]. Growing wafer size Graphene crystals also remains a topic for research. Graphene-based adsorption sensors and resonators are also highly researched topics. The presence of vibrational modes not there in 3-D materials invite interest for opto-mechanics. Graphene-based NEMS devices have the potential to be very sensitive detectors of mass and charge [2]. Graphene has also been explored for its high thermal conductivity applications. The area of defects and disorder in Graphene is a road less walked.

Recently, one of the primary focuses in Graphene research is bi-layer and multi-layer Graphene. It is again approached with a tight-binding approximation and is also a gapless material like mono-layer Graphene [14]. It was recently found that in bi-layers, the bandgap, unlike mono-layer, is tunable by an external electric field. The second layer can be stacked in different ways, in one of which, the second layer, can be twisted at an angle with respect to the first one. Twisted bi-layer Graphene involves strongly correlated electrons and is very sensitive to carrier density and the twist angle. Superconductivity has also been discovered with a *magic* twist angle of 1.1 degrees[4]. This has given rise to a new field named 'twistronics'. It is a very active topic for research with many potential applications in technology.

Appendix A

A.1 Numerical calculation of singular integrals

We can evaluate numerically a singular integral without changing the interval sizes by a method similar to Padé approximants. This method was inspired from [10, John and Singh]. We start by an integral of the type

$$I \;=\; \int_p^q \frac{A(y)}{B(y)} dy \tag{A.1}$$

that we wish to evaluate. We can divide the interval (q-p) into 'N' intervals of width $h = (q-p)/N$ and define :

$$I_n \;:=\; \int_{p+nh}^{p+(n+1)h} \frac{A(y)}{B(y)} dy \qquad \text{s.t. } n \;\in\; \{0, 1, \ldots\; N-1\} \tag{A.2}$$

Making the variable change $t \equiv (y-p)/h - \;n$ we have

$$I_n \;= h \int_0^1 \frac{A(\; p + (n+t)h)}{B(p + (n+t)h)}\; dt$$

For a given 'n', A(y) and B(y) are purely functions of 't'. Thus, for simplicity we can rewrite:

$$I_n \;=\; \int_0^1 \frac{A(t)}{B(t)}\; dt$$

Finally, invoking a second degree approximation for both the functions we get the following:

$$I_n \;\simeq h \int_0^1 \frac{dt^2 + et + f}{at^2 + bt + c}\; dt \tag{A.3}$$

where a,b,c,d,e and f are constants.

We can get a 'fit' for these constants by taking different values of t (equal to 0, 1/2 and 1) to get the following:

$$\begin{aligned} B(0) \;&=\; c \\ B\left(\tfrac{1}{2}\right) \;&=\; \frac{a}{4} + \frac{b}{2} + c \\ B(1) \;&=\; a + b + c \end{aligned}$$

We can simply calculate a, b and c to be the following:

$$\begin{aligned} a &= 2\left(B(0) - 2B\left(\tfrac{1}{2}\right) + B(1) \right) \\ b &= -B(1) + 4B(\tfrac{1}{2}) - 3B(0) \\ c &= B(0) \end{aligned}$$

And, the same process can be repeated for d, e and f.

Coming back to equation (A.3), the denominator can be written simply as

$$\begin{gathered} at^2 + bt + c = a(t - x_1)(t - x_2) \; ; \\ s.t. \\ x_1 x_2 = c/a \\ x_1 + x_2 = -b/a \end{gathered}$$

$$\Rightarrow I_n \simeq \frac{h}{a} \int_0^1 \frac{dt^2}{(t - x_1)(t - x_2)} + \frac{et}{(t - x_1)(t - x_2)} + \frac{f}{(t - x_1)(t - x_2)} \, dt \quad \text{(A.4)}$$

To ease our algebra we can define the following:

$$\begin{aligned} L &:= \int_0^1 \frac{dt}{(t - x_1)(t - x_2)} \\ &= \frac{1}{x_2 - x_1} \left\{ -\ln\left(1 - \frac{1}{x_1}\right) + \ln\left(1 - \frac{1}{x_2}\right) \right\} \end{aligned}$$

$$\begin{aligned} M &:= \int_0^1 \frac{t \; dt}{(t - x_1)(t - x_2)} \\ &= \ln\left(1 - \frac{1}{x_2}\right) + x_1 L \end{aligned}$$

$$\begin{aligned} N &:= \int_0^1 \frac{t^2 \; dt}{(t - x_1)(t - x_2)} \\ &= \int_0^1 dt + \int_0^1 \frac{x_2}{t - x_2} dt + x_1 M \\ &= 1 + x_2 \ln\left(1 - \frac{1}{x_2}\right) + x_1 M \end{aligned}$$

$$\Rightarrow I_n \simeq \frac{h}{a}(dN + eM + fL)$$

$$= \frac{h}{a} \left\{ d + dx_2 \ln\left(1 - \frac{1}{x_2}\right) + (dx_1 + e) \ln\left(1 - \frac{1}{x_2}\right) + (x_1(dx_1 + e) + f)L \right\}$$

which gives us our final result. Our integrand can turn singular, if either $a \simeq 0$ or $t = x_1, x_2$. In the former case, we can simply switch to a linear approximation for the denominator, and for the latter we can perform the calculations by 'going around' the singularity by adding a small imaginary part.
We have written the following Fortran 95 code which has been verified to work for standard integrals such as the semicircular density of states:

$$\int_{-1}^{1} \frac{\sqrt{1-z^2}}{z-0.9} dz$$

which turns singular at z=0.9.

The program file below can be found at this GitHub repo.

```
1   program singintquad
2   implicit none
3   integer, parameter :: dp=8
4   real(dp) :: lowlim, uplim
5   integer :: steps
6   complex(dp) :: integral
7
8   lowlim = 0.0_dp
9   uplim = 1.0_dp
10  steps=200  !keep steps so that interval width ~ 1.0e-2 to 1.0e-3
11
12  CALL integ13(nume,deno,lowlim,uplim,steps,integral)
13
14  write(*,'(A,2ES10.2e2,"i")') "The integral value is", integral
15  contains
16
17  subroutine integ13(num,den,q,p,N,integral)
18  !!!--------------------------
19  !This subroutine performs integration by equidistant intervals
     for
20  !'nearly' singular functions using quadratic approximations.
21  ! func -> function to integrate, q-> lower bound, p-> upper bound
     ,
22  !    N -> number of intervals (including q and p)
23  ! OUTPUT => integral
24  ! Use num, den to declare numerator, denominator respectively
25  !of the integral A(y)/B(y)
26  !!!--------------------------
27  real(dp), intent(in) :: q,p
28  integer, intent(in) :: N
29  real(dp) :: h,x
30  COMPLEX(dp) :: num,den, tp(3), int, a,b,c,d,e,f
31  COMPLEX(dp), intent(out) :: integral
32  integer :: i,k,t
33  h=(p-q)/N               ! h is the interval width.
34  x=(q+h/1000)            ! x tracks the interval.
35  integral=0.
36  k =0;t=0                 ! dummy indices
37  write(*,'(A,F7.3, " to", F7.3)') "Integral limits", q,p
38  write(*,'(A,ES8.2e2,/,A)') 'Interval width = ', h, repeat("-",10)
39
```

```
40  ! Main LOOP below
41  do i=0,N-1    !Variables named same as the writeup
42  int=0.
43  a =(2.) *(den(x+h)-2.*den(x+h/2) +den(x))
44  b = -den(x+h) + 4* den(x+h/2) -3*den(x)
45  c = den(x)
46  d =(2.) *(num(x+h)-2.*num(x+h/2) + num(x))
47  e = -num(x+h) - 3.*num(x) + 4.* num(x+h/2)
48  f = num(x)
49
50  if (abs(a) .le. 1.0e-6) then   ! leading coeff. too low, switch
     to linear
51  b = den(x+h)-den(x)
52  c = den(x)
53  if (abs(b) .le. 1.0e-3) then  !  log expansion, upto 3rd order.
54  int=h/(2*c) * (2*d/3 +e + 2*f-(2*b*e+b*f)/(3*c)+2*b**2 *f/(3*c
     **2))
55  k= k+1
56  else
57  int = h/(2*b**3) * (b*(-2*c*d+b*(d+2*e)) +2*( c**2 *d - b*c*e+b
     **2 *f)*log((1+b/c)) )
58  t=t+1
59  endif
60  else
61  tp(1)= ( -b + sqrt(b**2 - 4*a*c) )/(2*a) !x1
62  tp(2)= ( -b - sqrt(b**2 - 4*a*c) )/(2*a)  !x2
63  if ((real(tp(1)) < q .and. real(tp(1)) > p) .or. (real(tp(2)) < q
      .and. real(tp(2)) > p)) then
64  print*, "Quadratic approx not possible decrease interval to force
      linear"
65  EXIT
66  endif
67  ! int = h/a * ( d + log(1-1/tp(2)) *(d*(-b)/a +e+(d*tp(1)**2+e*tp
     (1)+f)/(tp(2)-tp(1))) &
68  !      - log(1-1/tp(1)) * (d*tp(1)**2+e*tp(1)+f)/(tp(2)-tp(1))  )
69  ! print*, 'quad', int, x
70  tp(1) = sqrt(4*a*c - b**2)
71  int = h*((4*a**2*atan((b+2*a)/tp(1))-4*a**2*atan(b/tp(1)))*f+(-b*
     tp(1)* &
72  log(abs(c+b+a))+b*tp(1)*log(abs(c))+(2*b**2-4*a*c)*atan((b+2*a)/
     tp(1))+(4*a*c-2*b**2)*&
73  atan(b/tp(1))+2*a*tp(1))*d+e*a*tp(1)*log(abs(c+b+a))-e*a*tp(1)*&
74  log(abs(c))-2*e*a*b*atan((b+2*a)/tp(1))+2*e*a*b*atan(b/tp(1)))
     /(2*a**2*tp(1))
75  endif
76
77  integral = int+integral
78  x=x+h
79  end do
80  write(*,'(A,I5,"/",I5)') "# log expansions in linear:", k,N
81  write(*,'(A,I5,"/",I5)') "# total linear approximations:", k+t,N
82  write(*,'(A,I5,"/",I5,/,A)') "# total quadratic approximations:",
      N-k-t,N, repeat("-",10)
83
84  end subroutine
85
```

```
86   function nume(x)
87   ! this is A(y) in integral(A(y)/B(y))
88   implicit none
89   COMPLEX(dp) :: nume,y
90   real(dp) :: x
91   y= complex(x,0.)
92   ! nume= complex(abs(x),0.)
93   ! nume = y-sqrt(y**2-1)
94   !nume = sqrt(1-y**2)
95   nume=1
96
97   return
98   end function nume
99
100  function deno(x)
101  ! this is B(y) in integral(A(y)/B(y))
102  implicit none
103  COMPLEX(dp) :: deno,y
104  real(dp) :: x
105  y = complex(x,0)
106  ! deno = complex(0.9-x,1.0e-10)
107  ! deno = sqrt(y**2 -1) + complex(0.,1.0e-10)
108  !deno = 1-y + complex(0.,1.0e-10)
109  deno = y**2
110
111  end function deno
112
113
114  end program singintquad
115
```

References

[1] K. S. Novoselov et al. "Two-dimensional atomic crystals". In: *Proceedings of the National Academy of Sciences* 102.30 (July 2005), pp. 10451–10453. DOI: 10.1073/pnas.0502848102. URL: https://doi.org/10.1073/pnas.0502848102.

[2] A. K. Geim and K. S. Novoselov. "The rise of graphene". In: *Nature Materials* 6.3 (Mar. 2007), pp. 183–191. DOI: 10.1038/nmat1849. URL: https://doi.org/10.1038/nmat1849.

[3] Neil Ashcroft. *Solid state physics*. New York: Holt, Rinehart and Winston, 1976. ISBN: 9780030839931.

[4] A. H. Castro Neto et al. "The Electronic Properties of Graphene". In: *Rev. Mod. Phys.* 81.1 (Jan. 14, 2009), pp. 109–162. ISSN: 0034-6861, 1539-0756. DOI: 10.1103/RevModPhys.81.109. arXiv: 0709.1163. URL: http://arxiv.org/abs/0709.1163.

[5] P. R. Wallace. "The Band Theory of Graphite". In: *Physical Review* 71.9 (May 1947), pp. 622–634. DOI: 10.1103/physrev.71.622. URL: https://doi.org/10.1103/physrev.71.622.

[6] Nathan O. Weiss et al. "Graphene: An Emerging Electronic Material". In: *Advanced Materials* 24.43 (Aug. 2012), pp. 5782–5825. DOI: 10.1002/adma.201201482. URL: https://doi.org/10.1002/adma.201201482.

[7] J. P. Hobson and W. A. Nierenberg. "The Statistics of a Two-Dimensional, Hexagonal Net". In: *Physical Review* 89.3 (Feb. 1953), pp. 662–662. DOI: 10.1103/physrev.89.662. URL: https://doi.org/10.1103/physrev.89.662.

[8] Rhyzik Gradshtein. *Table of integrals, series, and products*. Waltham, MA: Academic Press, 2015. ISBN: 978-0-12-384933-5.

[9] *Digital Library of Mathematical Functions,National Institute of Standards and Technology, U.S.* URL: https://dlmf.nist.gov/19.7.

[10] George C. John, J. E. Hasbun, and Vijay A. Singh. "Simple scheme for the numerical evaluation of nearly singular integrals". In: *Computers in Physics* 11.3 (1997), p. 293. DOI: 10.1063/1.168605. URL: https://doi.org/10.1063/1.168605.

[11] J. C. Slater and G. F. Koster. "Simplified LCAO Method for the Periodic Potential Problem". In: *Physical Review* 94.6 (June 1954), pp. 1498–1524. DOI: 10.1103/physrev.94.1498. URL: https://doi.org/10.1103/physrev.94.1498.

[12] S. Yu. Davydov. "Substitutional impurity in single-layer graphene: The Koster–Slater and Anderson models". In: *Semiconductors* 50.6 (June 2016), pp. 801–809. DOI: 10.1134/s106378261606004x. URL: https://doi.org/10.1134/s106378261606004x.

[13] Theanne Schiros et al. "Connecting Dopant Bond Type with Electronic Structure in N-Doped Graphene". In: *Nano Letters* 12.8 (July 2012), pp. 4025–4031. DOI: 10.1021/nl301409h. URL: https://doi.org/10.1021/nl301409h.

[14] Edward McCann. "Electronic Properties of Monolayer and Bilayer Graphene". In: *Graphene Nanoelectronics*. Springer Berlin Heidelberg, 2011, pp. 237–275. DOI: 10.1007/978-3-642-22984-8_8. URL: https://doi.org/10.1007/978-3-642-22984-8_8.